Available online at www.sciencedirect.com
ScienceDirect
Journal of Solid State Chemistry 181 (2008) 758–767
JOURNAL OF SOLID STATE CHEMISTRY
www.elsevier.com/locate/jssc

Synthesis of the titanium phosphide telluride Ti_2PTe_2: A thermochemical approach

Frauke Philipp[a], Peer Schmidt[a,*], Edgar Milke[b], Michael Binnewies[b], Stefan Hoffmann[c]

[a]*Inorganic Chemistry, Dresden University of Technology, Helmholtzstraße 10, 01069 Dresden, Germany*
[b]*Institute for Inorganic Chemistry, Leibniz University Hannover, Callinstr. 9, 30167 Hannover, Germany*
[c]*Max Planck Institute for Chemical Physics of Solids Dresden, Nöthnitzer Str. 40, 01187 Dresden, Germany*

Received 22 October 2007; received in revised form 21 December 2007; accepted 6 January 2008
Available online 10 January 2008

Abstract

The phosphide telluride Ti_2PTe_2 can be synthesised from the elements or from oxides in a thermite type reaction. Both ways have been optimised by consideration of the thermodynamic behaviour of the compound. Hence, the investigation of phase equilibria in the ternary system Ti/P/Te and of the thermal decomposition of Ti_2PTe_2 was necessary. This investigation was performed by using different experimental approaches as total pressure measurements, thermal analysis and mass spectrometry. The results were supported and further analysed by thermodynamic modelling of the ternary system. It was shown that $Ti_2PTe_{2(s)}$ decomposes to $Ti_2P_{(s)}$ and $Te_{2(g)}$ in six consecutive steps. The growth of single crystals of Ti_2PTe_2 is thermodynamically described as a chemical vapour transport with $TiCl_{4(g)}$ acting as the transport agent.

Keywords: Phosphide telluride; Thermal decomposition; Total pressure; Chemical vapour transport; Thermodynamic modelling

1. Introduction

Although many metal pnictide chalcogenides are known as antimonides selenides [1–5], antimonide tellurides [4–19], arsenides selenides [4,18–31], arsenides tellurides [18,30–37] and even phosphide sulphides [6,18,29,38–42] and phosphide selenides [4,18,23,40–42], by now there are only few phosphide tellurides: UPTe [43,44], IrPTe [45], OsPTe, RuPTe [46] and BaP_4Te_2 [47]. This must be due to the fact, that either no one ever tried to synthesise phosphide tellurides, or that the synthesis cannot be performed straightforward from the elements. Even the non-existence of a binary compound made up from phosphorus and tellurium shows that both elements cannot be combined easily. Anyhow, we succeeded in synthesising the compound Ti_2PTe_2, but the optimisation of this synthesis was possible only by consideration of the thermal behaviour of the compound. To understand the processes taking place, the thermodynamic properties of the ternary system Ti/P/Te have been investigated in detail as well by experimental methods as by thermodynamic modelling. The crystal structure and the physical properties of Ti_2PTe_2 will be presented soon [48].

2. Experimental part

Syntheses have been performed in evacuated closed silica tubes. Adherent moisture has been removed by heating under dynamic vacuum prior to use. Starting materials used were titanium powder (Alfa Aesar, 99.9%), tellurium (Acros, 99.8%), red amorphous phosphorus (Fluka, 99%, washed according to Ref. [49]), tellurium dioxide (Alfa Aesar, ultrapure), phosphorus pentoxide (Laborchemie Apolda, 99%, sublimed), tellurium oxide phosphate $Te_8O_{10}(PO_4)_4$ (synthesised according to Ref. [50]) and tellurium tetrachloride (synthesised from $Te_{(s)}$ and $Cl_{2(g)}$, sublimed). All starting materials have been handled in an argon-filled glove box ($c(O_2, H_2O) < 0.1$ ppm). Ti_2PTe_2 is not sensitive to oxygen and moisture and therefore was handled under air.

*Corresponding author. Fax: +49 351 463 37287;
URL: http://www.peer-schmidt.de.
E-mail address: peer.schmidt@chemie.tu-dresden.de (P. Schmidt).

0022-4596/$ - see front matter © 2008 Elsevier Inc. All rights reserved.
doi:10.1016/j.jssc.2008.01.003

Total pressure measurements were carried out in a silica zero-point membrane manometer as described in Ref. [51]. A point was recorded every 20 K while each point was recorded over 1 day, so that thermal equilibrium between solid phase and gas phase can be assured.

Thermogravimetric measurements have been performed under argon atmosphere on a Netzsch STA 449C with a heating rate of $10\,K\,min^{-1}$ in the temperature range from room temperature up to 1500 °C.

Investigations of the composition of the gas phase at the decomposition of Ti_2PTe_2 were performed using the mass spectrometer Varian MAT 212 coupled to a Knudsen-effusion cell. The sample was heated isothermally to 400, 600 and 800 °C. The evaporated species were ionised by electron impact ionisation with an energy of 70 eV and detected by a quadrupole mass spectrometer with $m/z \leqslant 350$.

Thermodynamic modelling of phase equilibria have been performed by using Calphad methods based on the Eriksson Gibss energy minimiser implemented in the programs Chemsage [52] and Tragmin [53]. The phase diagrams of the binary systems Ti/P and Ti/Te have been calculated with the *two dimensional phase mapping* mode (Chemsage [52]) in the temperature range 300–3000 K. The solid state–gas phase equilibria in the ternary and quaternary systems Ti/P/Te/(Cl) have been calculated (Tragmin [53]) at different given compositions isothermally in the temperature range 800–1300 K with $\Delta T = 100\,K$.

3. Results and discussion

3.1. Methods of synthesis

The compound Ti_2PTe_2 can be synthesised in two different ways. Besides a common solid state reaction from the elements under controlled thermal conditions (Eq. (1)), the reduction of either P_4O_{10} and TeO_2 or of the tellurium oxide phosphate $Te_8O_{10}(PO_4)_4$ [50] with elementary titanium to Ti_2O_3 and Ti_2PTe_2 (Eq. (2), respectively, (3)) leads to the aimed compound. Both ways show special advances towards the other one, so they can be used complementary.

$$2\ Ti_{(s)} + (1/4)\ P_{4(s,g)} + 2\ Te_{(l,g)} \rightarrow Ti_2PTe_{2(s)} \quad (1)$$

$$(19/3)\ Ti_{(s)} + (1/4)\ P_4O_{10(s,g)} + 2\ TeO_{2(s,g)} \rightarrow Ti_2PTe_{2(s)} + (13/6)\ Ti_2O_{3(s)} \quad (2)$$

$$(19/3)\ Ti_{(s)} + (1/4)\ Te_8O_{10}(PO_4)_{4(s)} \rightarrow Ti_2PTe_{2(s)} + (13/6)\ Ti_2O_{3(s)} \quad (3)$$

The reaction from the elements was carried out by heating the grinded educts in a silica tube of small volume (approximately 1 ml) up to 800 °C with a rate of $10\,K\,h^{-1}$, left at this temperature for 1 day and cooled down to 400 °C with a cooling rate of $1\,K\,h^{-1}$. This very slow cooling results in a long reaction time, but is necessary, as the heating temperature is at a point where the decomposition of the compound to the gas phase is already running and the rebuilding of Ti_2PTe_2 requires some time. Although no explicit kinetic studies were carried out no single-phase product was observed at higher cooling rates. In these cases, gaseous tellurium condenses out of thermodynamic equilibrium conditions. Anyway, at lower temperatures no formation of the compound could be observed.

The reduction of the oxides with titanium to form the goal compound Ti_2PTe_2 besides Ti_2O_3 can be considered as an example of a thermite reaction. The formation of the titaniumsesquioxide from elemental titanium lowers significantly the free Gibbs energy of the total reaction (2), respectively, (3) and therefore is the driving force for building Ti_2PTe_2 as a side product. The resulting free Gibbs energy for reaction (2) is $\Delta_R G^o_{1000\,K} = -2295\,kJ\,mol^{-1}$ compared to $\Delta_R G^o_{1000\,K} = -405\,kJ\,mol^{-1}$ for reaction (1); (used thermodynamic data are listed in Tables 1 and 2).

This kind of redox reaction is enabled by the difference in oxygen partial pressure between the titanium oxides and the tellurium, respectively, phosphorus oxides. As only one distinct partial pressure can exist above the reaction mixture, an equalisation is reached through the reaction. If also the gaseous species $P_4O_{6(g)}$ is concerned, it can be seen, that the level of this equalisation lies at Ti_2O_3 beside elemental tellurium and phosphorus (Fig. 1). In the sense of an electromotive series of solids there is a potential gradient between titanium and the tellurium and phosphorus oxides, which will be compensated by reaction (2); [54].

The advantage in using $Te_8O_{10}(PO_4)_4$ instead of TeO_2 and P_2O_5 is the retention of the wanted composition of the reaction mixture up to temperatures of 650 °C, while TeO_2 and even more P_2O_5 would be lost by sublimation at much lower temperatures.

The formed phosphide telluride can be separated from the oxide by chemical vapour transport from T_2 to T_1 ($T_2 > T_1$), e.g. from 1073 to 973 K by adding small amounts of $TeCl_{4(s)}$. The observed transport rate with approximately $0.02\,mg\,h^{-1}$ is that small, that this method is not convenient for synthesising large amounts of sample. On the other hand, it is very usable for growing single crystals for crystal structure determination and physical properties measurements [48].

3.2. Measurements of total pressure

The measured total pressure above solid Ti_2PTe_2 is shown logarithmically versus the inverse temperature in Fig. 2. At low temperatures, a slow increase of pressure can be seen. This is probably due to the evaporation of remaining elemental phosphorus (and eventually also tellurium) from the synthesis and thermal expansion of the gas phase. Around 600 °C, a sudden decrease of pressure appears. At this point, the reaction of the gas phase with the remaining starting material in completion of

Table 1
Thermodynamic data from the optimisation of solid compounds in the system Ti/P/Te/Cl

Compound	ΔH^{o}_{298K} (kJ mol^{-1})	ΔS^{o}_{298K} (J mol^{-1} K^{-1})	C_p (J mol^{-1} K^{-1})[a]			Reference
			a	*b*	*c*	
$Ti_{(s)}$	0	30.761	22.238	10.205	–0.008	[61]
$Te_{(s)}$	0	49.706	19.121	22.092		[61]
$P_{(red,s)}$	−17.489	22.803	16.736	14.895		[61]
$TeCl_{4(s)}$	−323.841	203.012	138.490			[61]
$TeO_{2(s)}$	−323.423	74.308	65.187	14.560	−0.502	[61]
$Ti_2O_{3(s)}$	−1520.884	77.253	53.070	163.444		[61]
$TiO_{2(rutile,s)}$	−944.747	50.626	73.346	3.054	−1.703	[61]
$Ti_3P_{(s)}$	−331.800	114.400	86.280	32.600		This work
$Ti_2P_{(s)}$	−321.600	83.700	64.140	22.300		This work
$Ti_7P_{4(s)}$	−1265.000	303.312	234.400	78.900		This work
$Ti_5P_{3(s)}$	−941.700	220.400	170.280	56.600		This work
$Ti_4P_{3(s)}$	−852.300	189.700	148.140	46.300		This work
$TiP_{(s)}$	−248.000	51.650	42.000	12.000		This work
$Ti_5Te_{4(s)}$	−621.240	351.000	187.700	139.400	0.040	This work
$Ti_3Te_{4(s)}$	−582.610	287.490	142.900	119.300		This work
$Ti_2Te_{3(s)}$	−397.090	208.210	101.600	87.000		This work
$TiTe_{2(s)}$	−196.620	136.380	60.400	54.300		This work
$Ti_2PTe_{2(s)}$	−447.988	183.800	99.474	79.491	−0.016	This work

[a] $C_p = a + b \times 10^{-3} T + c \times 10^{6} T^{-2}$.

Table 2
Thermodynamic data of gaseous compounds in the system Ti/P/Te/Cl

Compound	ΔH^{o}_{298K} (kJ mol^{-1})	ΔS^{o}_{298K} (J mol^{-1} K^{-1})	C_p (J mol^{-1} K^{-1})[a]			Reference
			a	*b*	*c*	
$Ti_{(g)}$	473.628	180.297	23.304	1.001		[61] C_p estimated
$TiCl_{2(g)}$	−237.232	278.345	60.124	2.218	−0.276	[61]
$TiCl_{3(g)}$	−539.317	316.838	87.257	−0.711	−1.293	[61]
$TiCl_{4(g)}$	−763.161	354.803	107.169	0.490	−1.050	[61]
$Te_{(g)}$	211.710	182.699	19.414	1.841	0.075	[61]
$Te_{2(g)}$	160.372	262.153	34.644	6.615	−0.025	[61]
$TeCl_{2(g)}$	−111.716	305.662	58.028	0.092	−0.331	[61]
$TeCl_{4(g)}$	−205.852	401.773	96.734	0.155	−0.548	[61]
$P_{(g)}$	333.883	163.201	20.669	0.172		[61]
$P_{2(g)}$	144.301	218.129	36.296	0.799	−0.414	[61]
$P_{4(g)}$	59.119	279.981	81.839	0.678	−1.343	[61]
$P_4O_{6(g)}$	−2214.290	345.745	216.355	8.665	−6.795	[61]
$P_4O_{10(g)}$	−2902.076	406.697	292.830	19.192	−10.715	[61]
$PCl_{3(g)}$	−286.922	311.984	82.366	0.406	−1.067	[61]
$PCl_{5(g)}$	−374.769	364.878	131.587	0.837	−1.778	[61]
$Cl_{2(g)}$	0	233.078	36.610	1.079	−0.272	[61]
$Cl_{(g)}$	121.294	165.184	23.736	−1.284	−0.126	[61]
$N_{2(g)}$	0	191.610	30.418	2.544	−0.238	[61]

[a] $C_p = a + b \times 10^{-3} T + c \times 10^{6} T^{-2}$.

the chemical equilibrium takes place, so that the total pressure is lowered. This observation reconfirms the fact found from experiments for synthesis optimisation, that high temperatures $\vartheta > 700\,^{\circ}C$ are needed for the formation of Ti_2PTe_2.

If one continues the measurement with increasing temperature, another rise of total pressure is observed starting from approximately 700 °C. This effect is finally due to the thermal decomposition of Ti_2PTe_2. It is not finished at 1000 °C, as it has not reached atmospheric pressure up to this temperature. Hence, you can find Ti_2PTe_2 beside TiP and small amounts of Ti_2Te_3 in the remaining solid phase after the measurement. This is a first hint, that Ti_2PTe_2 decomposes by release of $Te_{2(g)}$ or other tellurium-containing gaseous species. Thereby, the decomposition pressure of $Ti_2PTe_{2(s)}$ is lower than the one of pure $Te_{(s)}$ due to the stabilisation of the ternary phase relative to pure tellurium.

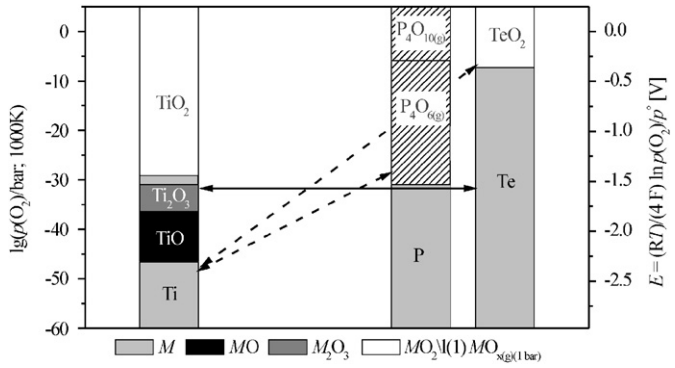

Fig. 1. Oxygen partial pressure and electrochemical potential above the oxides of titanium, tellurium and phosphorus calculated at 1000 K, marked: level of equalisation of oxygen partial pressure.

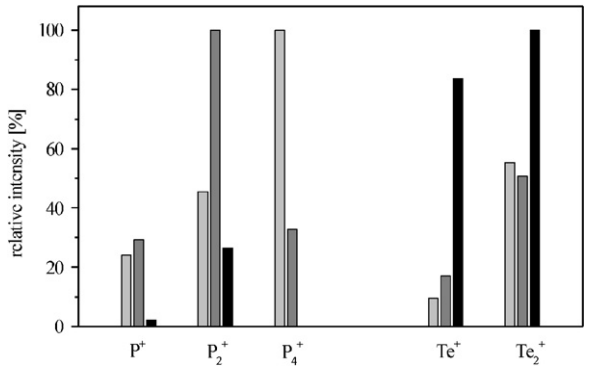

Fig. 3. Relative frequency of gaseous species detected by mass spectrometry after decomposition of Ti_2PTe_2 in a Knudsen-cell at 400 °C (■), 600 °C (■) and 800 °C (■).

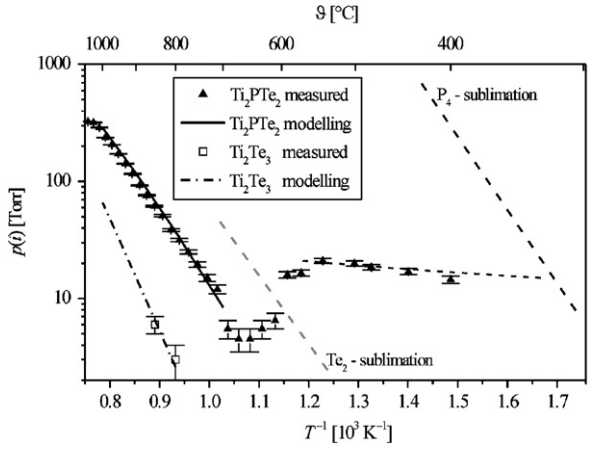

Fig. 2. Measured and modelled total pressure above solid Ti_2PTe_2 and Ti_2Te_3.

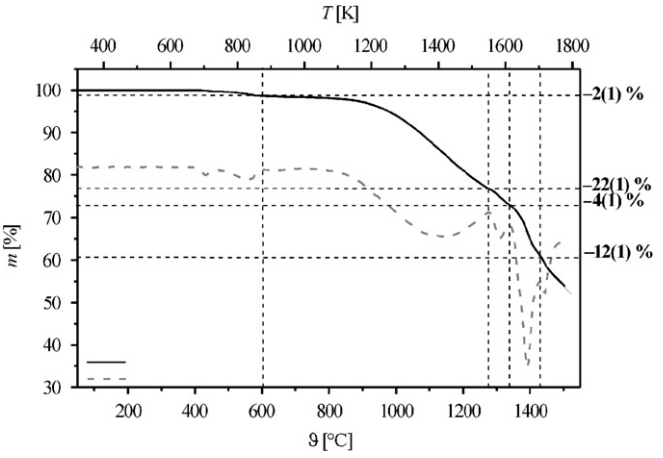

Fig. 4. Thermogravimetric decomposition of $Ti_2PTe_{2(s)}$; the dashed line shows the differential thermogravimetric curve.

As $TiP_{(s)}$ cannot be formed directly from $Ti_2PTe_{2(s)}$, only by delivery of $Te_{2(g)}$ to the gas phase, the decomposition must follow a more complex mechanism. This assumption is supported by the slow kinetics of the decomposition of Ti_2PTe_2, as equilibrium between solid phase and gas phase was only reached after 1 day.

3.3. Knudsen-cell mass spectrometry

To confirm that $Ti_2PTe_{2(s)}$ decomposes under release of tellurium-containing species and to investigate, if phosphorus-containing species are released simultaneously, the substance was pyrolised in a Knudsen-cell coupled to a mass spectrometer and the resulting gaseous molecules were examined. As the decomposition of Ti_2PTe_2 starts at 700 °C, only the gaseous species detected at 800 °C can be considered as decomposition products. Here, the most frequently found species is Te_2^+. Furthermore, high amounts of monoatomic Te^+ can be found, but only very few amounts of phosphorus-containing species (Fig. 3). This confirms, that the decomposition process of $Ti_2PTe_{2(s)}$ leads to the release of $Te_{2(g)}$ and $Te_{(g)}$, the amount of each distinct species is defined by the temperature dependent equilibrium between both of them.

The detection of as well phosphorus gas species as tellurium gas species at lower temperatures again is due to the evaporation of small amounts of remaining starting material from synthesis as it also was found in the total pressure measurements at low temperatures.

3.4. Thermogravimetric measurement

The thermogravimetric measurement shows in the first instance a very small mass loss of 2(1)% of the initial mass at temperatures up to 600 °C and a big decomposition step starting from approximately 650 °C, which is not finished at 1500 °C (Fig. 4). Up to this point, the mass loss is nearly 50(1)%. In agreement with the results of the measurement of total pressure and the mass spectrometry, the first mass loss can be explained by the evaporation of elemental phosphorus and tellurium. Hence, the molar mass of Ti_2PTe_2 is not treated as 100% but as 98% of the initial mass.

By regarding the differential thermogravimetric curve, the total decomposition step can be separated into several distinct steps. The first one ends close to 1300 °C and is coupled with a mass loss of 21(1)%. It can be explained by the formation of 1/3 Ti_3Te_4 + TiP per formula unit Ti_2PTe_2 and the release of 1/3 $Te_{2(g)}$ ($\Delta m/m_{theoretical} = -22\%$), (Eq. (4)). The next step gives another mass loss of 4(1)%. It can be explained by the phase width of TiP which is passed from the upper phase border ($TiP_{1.0}$) to the lower phase border ($TiP_{0.92}$) [55] by the release of 4/69 $Te_{2(g)}$ ($\Delta m/m_{theoretical} = -4\%$) as described in Eq. (5). Afterwards, another mass loss of 12(1)% is observed due to the formation of $Ti_4P_{3(s)}$ and 34/207 $Te_{2(g)}$ ($\Delta m/m_{theoretical} = -11\%$), while the remaining solid phase is made up of 2/9 Ti_3Te_4 + 1/3 Ti_4P_3 (Eq. (6)).

All described steps are consistent with the decomposition process obtained by the thermodynamic modelling of the ternary system Ti/P/Te, which will be regarded later on in this work. According to this modelling, the next step of decomposition has to be the formation of Ti_5P_3 besides Ti_3Te_4 (Eq. (6)), but this step is not completed at 1500 °C, when the gravimetric measurement was stopped. Anyway, the formation of $Ti_5P_{3(s)}$ was verified by means of X-ray powder diffraction in the residual from the thermogravimetric measurement.

$$Ti_2PTe_{2(s)} \rightleftharpoons (1/3)\ Ti_3Te_{4(s)} + TiP_{(s)} + (1/3)\ Te_{2(g)} \quad (4)$$

$$(1/3)\ Ti_3Te_{4(s)} + TiP_{(s)} \rightleftharpoons (7/23)\ Ti_3Te_{4(s)} + (25/23)\ TiP_{0.92(s)} + (4/69)\ Te_{2(g)} \quad (5)$$

$$(7/23)\ Ti_3Te_{4(s)} + (25/23)\ TiP_{0,92(s)} \rightleftharpoons (2/9)\ Ti_3Te_{4(s)} + (1/3)\ Ti_4P_{3(s)} + (34/207)\ Te_{2(g)} \quad (6)$$

$$(2/9)\ Ti_3Te_{4(s)} + (1/3)\ Ti_4P_{3(s)} \rightleftharpoons (1/9)\ Ti_3Te_{4(s)} + (1/3)\ Ti_5P_{3(s)} + (2/9)\ Te_{2(g)} \quad (7)$$

3.5. Thermodynamic modelling of the binary systems Ti/P and Ti/Te

To understand the complex mechanism of formation and decomposition of Ti_2PTe_2 and to optimise the synthesis of this and other phosphide tellurides, a detailed thermodynamic modelling and description of the ternary system Ti/P/Te was aspired. In this modelling, at least some of the numerous binary titanium phosphides and -tellurides had to be included, to reach a realistic picture of the phase relations in the ternary system. Since thermodynamic data for the binary compounds have only fragmentary been reported afore, an estimation and adjustment of these data by modelling of the binary systems Ti/P and Ti/Te was performed using the program Chemsage [52]. Using this program, thermodynamic data of all included solid phases and of the liquid phase have been varied that way that known thermic effects of the compounds as melting points, eutectica and peritectica could be represented correctly in comparison with literature data [55,56]. All optimised data have been introduced into the modelling of the ternary system Ti/P/Te, adjusted to experimental observations for this system and reoptimised in modelling of the binary systems, until the whole set of data was consistent with all experimental results.

In the system Ti/Te, standard enthalpies and entropies of formation were known for the compounds $TiTe_{2(s)}$ and $Ti_2Te_{3(s)}$ and for a compound having the nominal composition $TiTe_{(s)}$, but being noted for showing a wide homogeneity range [57]. As there is not such a phase in the published phase diagram, which was used for comparison [55], the standard entropy published for $TiTe_{(s)}$ multiplied by five, have been used to describe the compound $Ti_5Te_{4(s)}$. The enthalpy of formation for this compound has been determined by heat flow calorimetry [58]. For the last binary titanium telluride $Ti_3Te_{4(s)}$, no data at all have been accessible, so they are newly estimated here. The calculated phase diagram is in good agreement with the experimental one [55] concerning the thermal effects of $Ti_{(s)}$, $Ti_5Te_{4(s)}$, $TiTe_{2(s)}$ and $Te_{(s)}$ (Fig. 5); the melting point of $Ti_4Te_{3(s)}$ is unknown. The obtained thermodynamic data for the system Ti/Te are listed in Table 3.

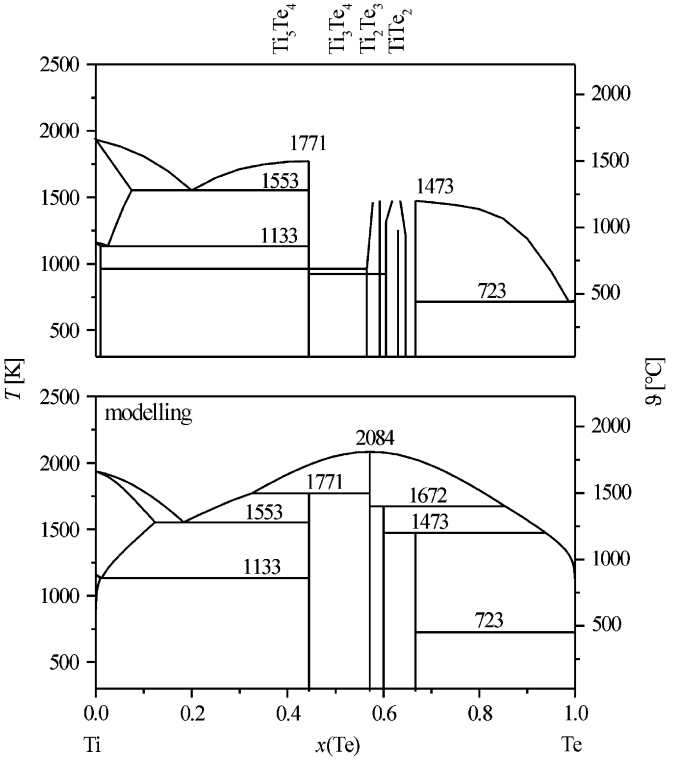

Fig. 5. Phase diagram of the binary system Ti/Te as published [55] (top) and as resulted from thermodynamic modelling using the program Chemsage [52] (bottom).

Table 3
Thermodynamic data for the system Ti/Te yield from the modelling in comparison to literature [57,58]

	ΔH^{o}_{298K} (kJ mol^{-1})		$\Delta S^{o}_{298\,K}$ (J K^{-1} mol^{-1})	
	Optimisation	Literature	Optimisation	Literature
$TiTe_{2(s)}$	−196.62	−213.1 [57]	136.38	117.2 [57]
$Ti_2Te_{3(s)}$	−397.09	−355±40 [57]	208.21	207±25 [57]
$Ti_3Te_{4(s)}$	−582.61	–	287.49	–
$Ti_5Te_{4(s)}$	−621.24	−605±100[a] [57] −630±10 [58]	351.00	420±40[a] [57]

[a] $5 \cdot TiTe_{(s)}$: "wide homogeneity range" [57].

In the system Ti/P, far less thermodynamic data have been known in advance to this work. The existence of the compounds Ti_3P, Ti_2P, Ti_7P_4, Ti_5P_3, Ti_4P_3, TiP and TiP_2 is shown in the phase diagram [56], but only the enthalpy of formation for $TiP_{(s)}$ has been determined on two different ways to −265 kJ mol^{-1}, respectively, to −324 kJ mol^{-1} [59]. As there is not even an existence range determined for TiP_2, this compound was excluded from modelling. For all other compounds, the entropies of formation have been estimated according to the Neumann–Kopp rule [60] as the sum of the entropies of elemental titanium and red phosphorus. For the enthalpies of formation normalised to one phosphorus atom per formula unit a linear devolution from $Ti_{(s)}$ to $TiP_{(s)}$ with increasing phosphorus content was assumed and used as a starting point.

Neither for any titanium telluride nor for the titanium phosphides the functions of heat capacity were known, so these were estimated for all compounds again according to the Neumann-Kopp rule.

The experimental phase diagram [56] for the system Ti/P is covered by the calculated very well (Fig. 6), the gained data are presented in Table 4.

3.6. Thermodynamic modelling of the ternary system Ti/P/Te

Using the optimised thermodynamic data for the binary titanium phosphides and tellurides, solid state–gas phase equilibria in the ternary system Ti/P/Te have been modelled using the program Tragmin [53]. In Tragmin, there is a limit of the number of solid phases; hence, only the phosphides $TiP_{(s)}$, $Ti_5P_{3(s)}$ and $Ti_2P_{(s)}$ and the tellurides $TiTe_{2(s)}$, $Ti_2Te_{3(s)}$ and $Ti_3Te_{4(s)}$ were included besides $Ti_2PTe_{2(s)}$ and the elements $Ti_{(s)}$, $Te_{(s)}$ and $P_{(red,s)}$.

As already described, the modelling was done in alternation with the modelling of the binary systems, so that experimental results could be reproduced for both binary systems and the ternary one. Not until this agreement was reached, new results were considered. First of all, the agreement between model and experiment was proved on the measurement of total pressure. Finally the model was able to reflect the total pressure above solid Ti_2PTe_2 and Ti_2Te_3 very well (Fig. 2).

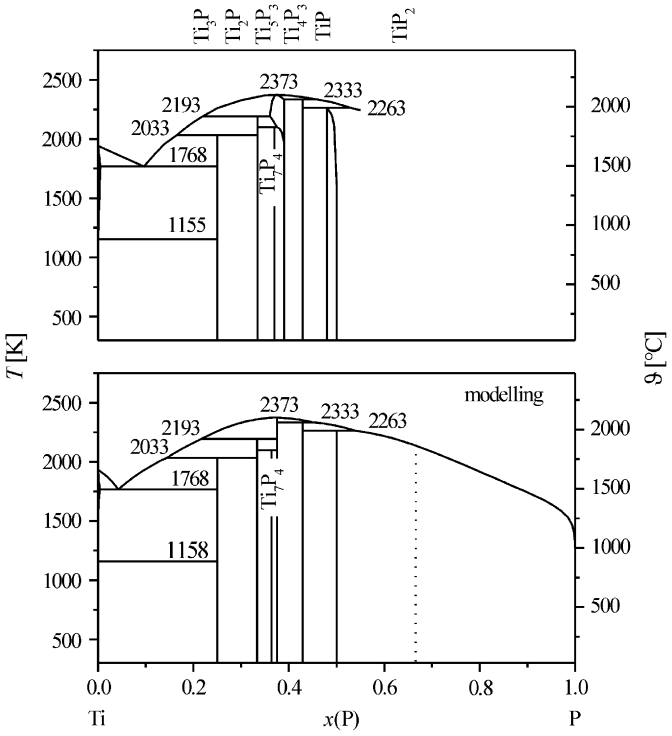

Fig. 6. Phase diagram of the binary system Ti/P as published [56] (top) and as resulted from thermodynamic modelling using the program Chemsage [52] (bottom).

Table 4
Thermodynamic data for the system Ti/P yield from the modelling in comparison to literature [57,59]

	ΔH^{o}_{298K} (kJ mol^{-1})		$\Delta S^{o}_{298\,K}$ (J K^{-1} mol^{-1})	
	Optimisation	Literature	Optimisation	Literature
$TiP_{(s)}$	−248.0	−265.3 −324	51.65	–
$Ti_4P_{3(s)}$	−852.3	–	189.7	–
$Ti_5P_{3(s)}$	−941.7	–	220.4	–
$Ti_7P_{4(s)}$	−1265.0	–	303.32	–
$Ti_2P_{(s)}$	−321.6	–	83.7	–
$Ti_3P_{(s)}$	−331.8	–	114.4	–

Fig. 7 shows the resulting ternary phase diagram with all appearing coexistence ranges. The ternary areas $Ti_2PTe_{2(s)}$/$Ti_2Te_{3(s)}$/$TiP_{(s)}$ and $Ti_2PTe_{2(s)}$/$Te_{(s)}$/$TiP_{(s)}$ have also been proved by solid-state reactions. If the decomposition of $Ti_2PTe_{2(s)}$ runs by the release of $Te_{2(g)}$, as shown by mass spectrometry, the composition of the solid phase has to follow the dashed line until finally $Ti_2P_{(s)}$ remains. Each time it crosses a solid line and therewith enters a new coexistence range, another decomposition step takes place. As the phase width of $TiP_{(s)}$ was not incorporated in the modelling, the passing through its phase region as found in the thermogravimetric measurement cannot be seen here. So, the presented phase diagram shows the decomposition of $Ti_2PTe_{2(s)}$ in six steps, if also the existence of $Ti_4P_{3(s)}$ and $Ti_7P_{4(s)}$ between $TiP_{(s)}$ and $Ti_2P_{(s)}$ is considered. These steps

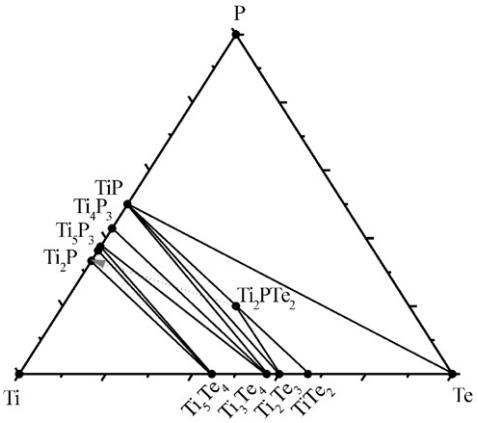

Fig. 7. Calculated phase diagram ($T = 1000$ K) of the system Ti/P/Te-calculation using the program Tragmin [53], (···) decomposition of Ti_2PTe_2 under release of $Te_{2(g)}$.

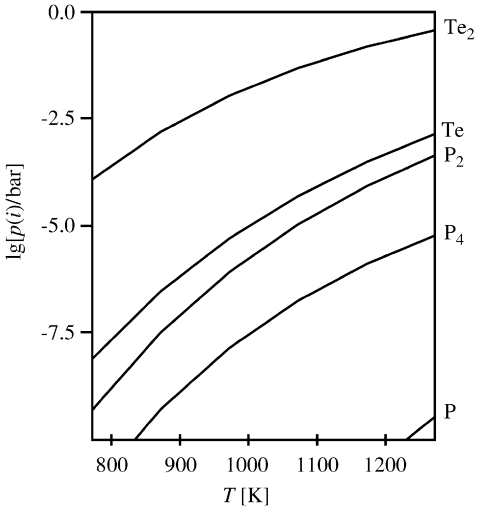

Fig. 8. Calculated composition of the gas phase above solid Ti_2PTe_2-calculation using the program Tragmin [53].

can be described by the Eqs. (8)–(13), which give in sum the total decomposition to $Ti_2P_{(s)}$ and $Te_{2(g)}$ (14). It is remarkable for this process, that most of the steps are not typical decomposition reactions in that one compound decays into another one plus a gaseous species. These steps detail reactions in that a new compound is built from two starting compounds, while a gaseous side product is released. This explains the very slow progress of the whole decomposition process.

$$Ti_2PTe_{2(s)} \rightleftharpoons (1/2)\ Ti_2Te_{3(s)} + TiP_{(s)} + (1/4)\ Te_{2(g)} \quad (8)$$

$$(1/2)\ Ti_2Te_{3(s)} \rightleftharpoons (1/3)\ Ti_3Te_{4(s)} + (1/12)\ Te_{2(g)} \quad (9)$$

$$(1/9)\ Ti_3Te_{4(s)} + TiP_{(s)} \rightleftharpoons (1/3)\ Ti_4P_{3(s)} + (2/9)\ Te_{2(g)} \quad (10)$$

$$(1/9)\ Ti_3Te_{4(s)} + (1/3)\ Ti_4P_{3(s)} \rightleftharpoons (1/3)\ Ti_5P_{3(s)} + (2/9)\ Te_{2(g)} \quad (11)$$

$$(1/36)\ Ti_3Te_{4(s)} + (1/3)\ Ti_5P_{3(s)} \rightleftharpoons (1/4)\ Ti_7P_{4(s)} + (1/18)\ Te_{2(g)} \quad (12)$$

$$(1/12)\ Ti_3Te_{4(s)} + (1/4)\ Ti_7P_{4(s)} \rightleftharpoons Ti_2P_{(s)} + (1/6)\ Te_{2(g)} \quad (13)$$

$$\sum Ti_2PTe_{2(s)} \rightleftharpoons Ti_2P_{(s)} + Te_{2(g)} \quad (14)$$

In comparison to the decomposition steps found from thermogravimetric measurements, the first measured step covers equilibria (8) and (9). The second step originates from passing through the phase width of $TiP_{(s)}$, which is not included in the modelling. So the second and third thermogravimetrically measured step can be assigned to equation (10). The thermogravimetric measurement was stopped at 1500 °C. At this temperature, the fourth decomposition step (equation (11)) is taking place; hence, $Ti_5P_{3(s)}$ can be found in the residual. In contrast, in the total pressure measurement up to 1000 °C, only reaction (8) takes place, so $TiP_{(s)}$ is found afterwards. The composition

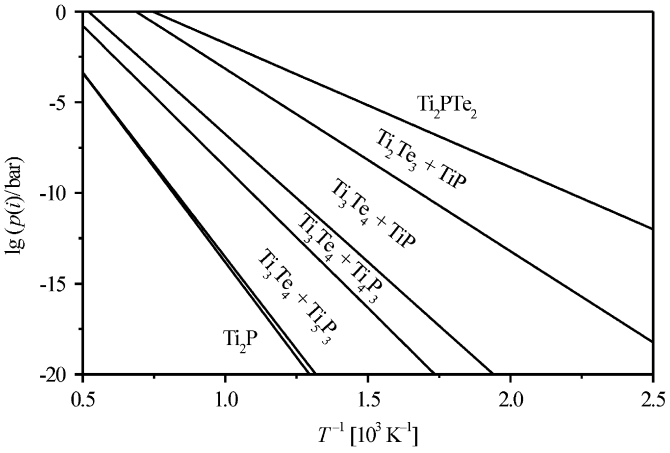

Fig. 9. Tellurium partial pressures $p(i)$, ($i = Te_{2(g)}$) above all coexistence lines subtended during the decomposition of $Ti_2PTe_{2(s)}$ to $Ti_2P_{(s)}$ and $Te_{2(g)}$, unmarked area: $Ti_3Te_{4(s)} + Ti_7P_{4(s)}$-calculation using the program Tragmin [53].

of the gas phase above solid Ti_2PTe_2 as obtained from complex modelling of the phase equilibria is shown in Fig. 8. Here the dominance of the species $Te_{2(g)}$ and $Te_{(g)}$ versus the phosphorus species can be seen, as it was found by mass spectrometry. Nevertheless, the dissociation of $Te_{2(g)}$ in the regarded temperature range creates a partial pressure $p(Te_{(g)})$ three orders of magnitude lower than $p(Te_{2(g)})$. Therefore the contribution of the dissociation can be neglected in calculations of the free Gibbs energy of reactions (8)–(14).

In Fig. 9, the tellurium pressure for equilibria (8)–(13) according to equation (15) above the distinct coexistence ranges is shown. Here, the same sequence of phases can be seen which confirms the decomposition process (8)–(13).

$$lg\, p(Te_2) = \frac{-\Delta_R H^o}{2.303\, R\, T} + \frac{\Delta_R S^o}{2.303\, R}. \quad (15)$$

3.7. Thermodynamic modelling of the chemical vapour transport of Ti_2PTe_2

Subsequent to the ternary system Ti/P/Te modelling of the quaternary system Ti/P/Te/Cl has been performed to investigate the mechanism of the chemical vapour transport. Therefore, chlorine-containing gaseous species and solid $TeCl_4$ were included in addition to the same species as regarded in the ternary system. Fig. 10 shows the gas phase above the area $Ti_2PTe_{2(s)}/Ti_2Te_{3(s)}/TiP_{(s)}/TeCl_{4(s)}$. It can be seen easily, that $TiCl_{4(g)}$ is built from the starting compounds and exhibits a very high partial pressure. If the region down to a pressure of 10^{-5} bar is regarded, the tellurium-containing species $Te_{2(g)}$, $Te_{(g)}$ and $TeCl_{2(g)}$ and the phosphorus-containing species $P_{2(g)}$ can be found. This region is said to be relevant for chemical transport reactions, so the basic condition for a chemical transport of $Ti_2PTe_{2(s)}$ is fulfilled. But beside a sufficient partial pressure for each component, it is necessary, that the solubility of each component in the gaseous phase is temperature dependent at such a rate that the direction of the transport equilibrium can be changed by a moderate temperature gradient. To check this possibility, the transport efficiency was examined. It is defined as the difference of partial pressure between source and sink normalised to the solvent. According to this definition, a transport agent should show negative values for the transport efficiency, as it gets consumed in the source and released in the sink, and transport-relevant species should show positive values of transport efficiency.

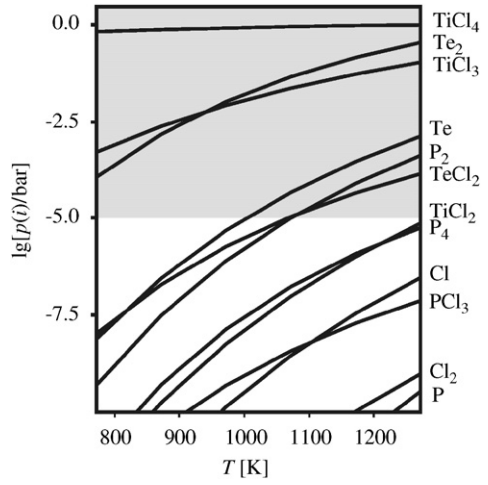

Fig. 10. Calculated composition of the gas phase $p(i) = f(T)$ above a solid mixture $Ti_2PTe_{2(s)}/Ti_2Te_{3(s)}/TiP_{(s)}/TeCl_{4(s)}$-calculation using the program Tragmin [53], grey marked area: transport relevant region.

In a first result, the calculation of transport efficiency shows only $TiCl_{4(g)}$ as transport agent and $TiCl_{3(g)}$ and $Te_{2(g)}$ as transport relevant species (Fig. 11, left). That way the chemical transport of $Ti_2PTe_{2(s)}$ would not be possible, as there would be no transport of phosphorus. Only by regarding very low transport efficiencies, a transport relevance of $P_{2(g)}$ can be seen (Fig. 11, right). This very low transport efficiency of $P_{2(g)}$ fits to the very low transport rate which was found experimentally ($\Delta m/t = 0.02\,\mathrm{mg\,h^{-1}}$). However, the chemical transport of $Ti_2PTe_{2(s)}$ is possible and can be described by Eq. (16). Moreover, the modelling shows that $TiTe_{2(s)}$ is transported simultaneously to $Ti_2PTe_{2(s)}$ according to Eq. (17).

$$2\ Ti_2PTe_{2(s)} + 12\ TiCl_{4(g)} \rightleftharpoons 16\ TiCl_{3(g)} + 2\ Te_{2(g)} + P_{2(g)} \tag{16}$$

$$TiTe_{2(s)} + 3\ TiCl_{4(g)} \rightleftharpoons 4\ TiCl_{3(g)} + Te_{2(g)} \tag{17}$$

In both transport reactions, $TiCl_{4(g)}$ acts as the transport agent. In the experiment, it is built from the reaction mixture immediately, although solid $TeCl_4$ was added. This reaction proceeds to reach an equalisation in chlorine partial pressure. The tellurium chlorides $TeCl_{4(g)}$ and $TeCl_{2(g)}$—and as well the phosphorus chlorides $PCl_{5(g)}$ and $PCl_{3(g)}$—have no common existence range with elemental titanium, so they cannot coexist (Fig. 12). By

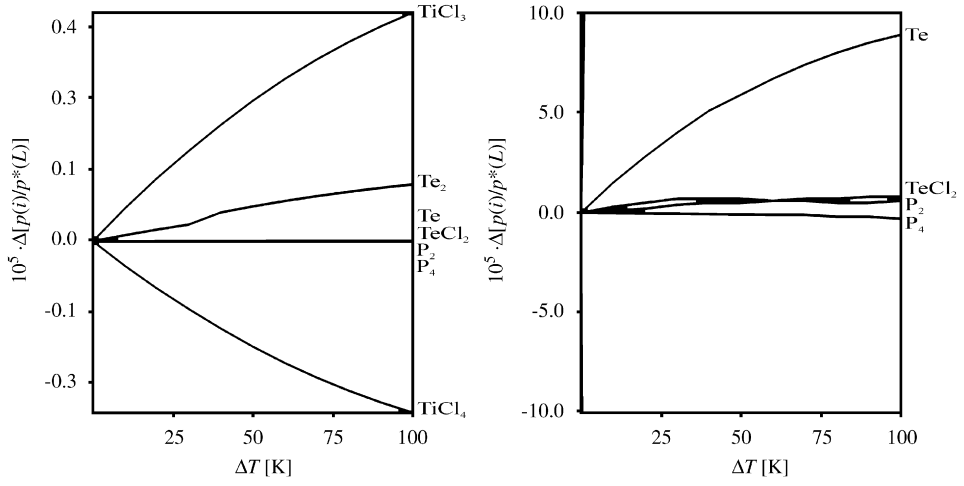

Fig. 11. Transport efficiency $\Delta(p(i)/p^*(L))$ above a solid mixture $Ti_2PTe_{2(s)}/Ti_2Te_{3(s)}/TiP_{(s)}/TeCl_{4(s)}$-calculation using the program Tragmin [53], the right side shows the limiting efficiency of $P_{2(g)}$ for the chemical transport of $Ti_2PTe_{2(s)}$.

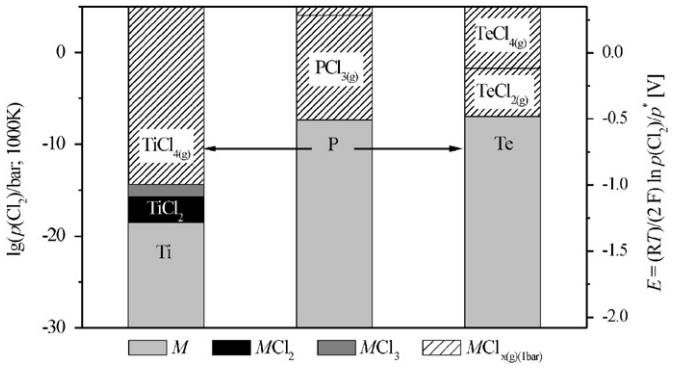

Fig. 12. Chlorine partial pressure $\lg(p(Cl_2)/\text{bar})$ and electrochemical potential E at $T = 1000\,K$ above the chlorides of titanium, tellurium and phosphorus, marked: level of equalisation of chlorine partial pressure.

the oxidation of titanium to $TiCl_{4(g)}$ and the reduction of $TeCl_{4(g)}$, a shared range of existence can be reached, analogical to the description of the redox processes in the oxidic system. Likewise, the use of phosphorus chlorides or even elemental chlorine would lead to the formation of $TiCl_{4(g)}$, so it is possible to use the most practicable chlorine supplying agent, which here is solid $TeCl_4$.

4. Conclusion

By combination of all the methods described above, the thermodynamic conditions in the system Ti/P/Te can be understood. Thereby, the difficulties in the synthesis of the ternary compound Ti_2PTe_2 from the elements can be assigned to three effects:

The process of phase formation and decomposition is quite complex and includes the formation of different stable binary phases.

As found experimentally, the kinetics of the building reaction are too slow at temperatures below 700 °C and no formation of the compound could be observed. Therefore, you have to work at higher temperatures where the decomposition reaction of the wanted compound already is running and to cool down slowly afterwards. At higher cooling rates, gaseous tellurium condenses out of thermodynamic equilibrium conditions.

At last, it is absolute necessary to control the composition and the pressure of the gas phase by the chosen conditions, as both phosphorus and tellurium exhibit high vapour pressures already at low temperatures. This can be overcome by using a small reaction volume and a defined temperature gradient so that the gas phase recondenses on the residual solid.

An easier way to yield Ti_2PTe_2 is by reducing TeO_2 and P_2O_5 or better $Te_8O_{10}(PO_4)_4$ with elemental titanium in a thermite-type reaction. Due to the formation of Ti_2O_3, the Gibbs free energy of this reaction is very low, so the driving force for this reaction is much higher. But here the products have to be separated. This is possible by chemical vapour transport of Ti_2PTe_2 with $TiCl_{4(g)}$, which shows very low transport rates due to the low partial pressure of $P_{2(g)}$, the only transport relevant species for phosphorus.

Finally, the results cannot be passed on directly to the synthesis of other ternary phosphide tellurides M_xPTe_y, as the distinct conditions have to be regarded individually for each system. Especially the basic binary systems M/P and M/Te have to be taken into account. The synthesis from the oxides should be applicable for every metal that can form an oxide, whose oxygen partial pressure is below the one of $P_4O_{6(g)}$, that means in the same range as the one of $Ti_2O_{3(s)}$. But, still a suitable way of separating the aimed compound from the oxide, e.g. by chemical transport has to be found.

Acknowledgments

The authors thank Mrs. S. Müller, Max Planck Institute for Chemical Physics of Solids, Dresden, for performing the thermogravimetric measurements and Mrs. J. Krug, Dresden University of Technology, for help with the synthesis. Financial support by the Deutsche Forschungsgemeinschaft is gratefully acknowledged.

References

[1] H. Kleinke, B. Harbrecht, Z. Anorg. Allg. Chem. 625 (1999) 1873.
[2] H. Kleinke, Chem. Commun. 2000 (2000) 1941.
[3] H. Kleinke, J. Alloys Compd. 336 (2002) 132.
[4] A.J. Foecker, W. Jeitschko, J. Solid State Chem. 162 (2001) 69.
[5] T.K. Reynolds, J.G. Bales, F.J. DiSalvo, Chem. Mater. 14 (2002) 4746.
[6] A.J. Klein Haneveld, F. Jellinek, J. Less Common Met. 18 (1969) 123.
[7] P. Jensen, A. Kjekshus, J. Less Common Met. 13 (1967) 357.
[8] K. Deneke, A. Rabenau, Z. Anorg. Allg. Chem. 333 (1964) 201.
[9] R.L. Stegmann, E.A. Peretti, J. Inorg. Nucl. Chem. 28 (1966) 1589.
[10] S.S. Abdul Noor, J. Appl. Phys. 61 (1987) 3549.
[11] F.K. Lotgering, E.W. Gorter, J. Phys. Chem. Solids 3 (1957) 238.
[12] J. Rossat-Mignod, P. Burlet, S. Quezel, J.M. Effantin, D. Delacote, H. Bartholin, O. Vogt, D. Ravot, J. Magn. Magn. Mater. 31 (1983) 398.
[13] Y.C. Wang, K.M. Poduska, R. Hoffmann, F.J. DiSalvo, J. Alloys Compd. 314 (2001) 132.
[14] T.K. Reynolds, R.F. Kelley, F.J. DiSalvo, J. Alloys Compd. 366 (2004) 136.
[15] M.N. Abdusalyamova, A.G. Chuiko, A.Yu. Golubkov, S.I. Popov, L.S. Parfenova, A. Prokofiev, I.A. Smirnov, J. Alloys Compd. 205 (1994) 107.
[16] W.-S. Kim, G.Y. Chao, Can. Mineral. 29 (1991) 401.
[17] P. Terzieff, H. Ipser, Monatsh. Chem. 123 (1992) 35.
[18] F. Hulliger, Mater. Res. Bull. 14 (1979) 259.
[19] R. Ferro, Z. Anorg. Allg. Chem. 275 (1954) 320.
[20] H.J. Whitfield, J. Solid State Chem. 39 (1981) 209.
[21] F. Hulliger, Z. Naturforsch. B 36 (1981) 463.
[22] F. Hulliger, T. Siegrist, Mater. Res. Bull. 16 (1981) 1245.
[23] A. Kjekshus, T. Rakke, Acta Chem. Scand. A 33 (1979) 609.
[24] J. Leciejewicz, A. Zygmunt, Phys. Status Solidi A 13 (1972) 657–660.
[25] R.M. Imamov, I.I. Petrov, Kristallografiya 13 (1968) 412.
[26] A. Kjekshus, W.E. Jamison, Acta Chem. Scand. 25A (1971) 1715.
[27] H. Hahn, D. Thiele, Z. Anorg. Allg. Chem. 303 (1960) 147.
[28] R.B. Beeken, J.W. Schweitzer, Phys. Rev. B 23 (1981) 3620.
[29] F. Hulliger, G.W. Hull Jr., Solid State Commun. 8 (1970) 1379.
[30] A. Wojakowski, J. Less Common Met. 107 (1985) 155.

[31] D. Pietraszko, K. Lukaszewicz, Bulletin de l'academie Polonaise des Sciences, Serie des Sciences 23 (1975) 337.
[32] A. Mosset, Y.P. Jeannin, J. Less Common Met. 26 (1972) 285.
[33] W. Bensch, W. Heid, J. Alloys Compd. 224 (1995) 220.
[34] C.-C. Wang, C. Eylem, T. Hughbanks, Inorg. Chem. 37 (1998) 390.
[35] A. Mosset, Y.P. Jeannin, J. Solid State Chem. 7 (1973) 124.
[36] F.Q. Huang, P. Brazis, C.R. Kannewurf, J.A. Ibers, Inorg. Chem. 39 (2000) 3176.
[37] F.Q. Huang, C. Flaschenriem, P. Brazis, C.R. Kannewurf, J.A. Ibers, Inorg. Chem. 42 (2003) 3194.
[38] F. Hulliger, R. Schmelczer, D. Schwarzenbach, J. Solid State Chem. 21 (1977) 371.
[39] F. Hulliger, J. Less Common Met. 16 (1968) 113.
[40] R. Wawryk, A. Wojakowski, A. Pietraszko, Z. Henkie, Solid State Commun. 133 (2005) 295.
[41] W. Jeitschko, Acta Cryst. B 30 (1974) 2565.
[42] P.C. Donohue, P.E. Bierstedt, Inorg. Chem. 8 (1969) 2690.
[43] A. Zygmunt, A. Murasik, S. Ligenza, J. Leciejewicz, Phys. Status Solidi A 22 (1974) 75.
[44] W.B. Pearson, Z. Kristallogr. 171 (1985) 23.
[45] G. Kliche, Z. Naturforsch. 41b (1986) 130.
[46] H.D. Lutz, Th. Schmidt, G. Wäschenbach, Z. Anorg. Allg. Chem. 562 (1988) 7.
[47] S. Jörgens, D. Johrendt, A. Mewis, Chem. Eur. J. 9 (2003) 2405.
[48] F. Philipp, P. Schmidt, M. Ruck, W. Schnelle, J. Solid State Chem., submitted.
[49] G. Brauer, Handbuch der Präparativen Anorganischen Chemie, Bd. 1, S. 506, 3. Auflage, F. Enke Verlag Stuttgart, 1975.
[50] H. Mayer, G. Pupp, Z. Kristallogr. 145 (1977) 321.
[51] H. Oppermann, O. Schneider, E. Wittig, Chemische Technik 18 (7) (1966) 433.
[52] G. Eriksson, K. Hack, M. Philipps, C. Fullerton-Batten, ChemSage Version 4.2—Gibbs Energy Minimizer and Optimization Routine,, GTT Technologies, Herzogenrath, 2000.
[53] G. Krabbes, W. Bieger, K.-H. Sommer, T. Söhnel, GMIN-Version 4.01-program package TRAGMIN for calculation of phase equilibria, IFW Dresden, TU Dresden, 1994.
[54] P. Schmidt, Prog. Solid State Chem., (Habilitation TU Dresden: http://hsss.slub-dresden.de/deds-access/hsss.urlmapping.MappingServlet?id=1200397971615-4054) in preparation.
[55] H. Cordes, R. Schmid Fetzer, J. Alloys Compd. 216 (1994) 197.
[56] J.L. Murray, Binary Alloy Phase Diagrams, vol. 3, second ed., T.B. Massalski (Ed.), ASM International Materials Park, Ohio, 1990, p. 2989.
[57] O. Kubaschewski, At. Energy Rev.: Thermochem. Prop. 9 (1983).
[58] O.Yu. Pankratova, N.Yu. Bobrovskayqa, R.A. Zvinchuk, Fizika, Khimiya 3 (1995) 80.
[59] M.E. Schlesinger, Chem. Rev. 102 (2002) 4267.
[60] Compare H. Oppermann, P. Schmidt, Z. Anorg. Allg. Chem. 631 (2005) 1309.
[61] O. Knacke, O. Kubaschewski, K. Hesselmann, Thermochemical Properties of Inorganic Substances, second ed., Springer, 1991.